Inorg. Chem. **2006**, *45*, 1463–1470

Synthesis and Electrochemistry of Undeca-substituted Metallo-benzoylbiliverdins

Owendi Ongayi,[†] M. Graça H. Vicente,*[,†] Zhongping Ou,[‡] Karl M. Kadish,*[,‡] M. Ravi Kumar,[†] Frank R. Fronczek,[†] and Kevin M. Smith*[,†]

Department of Chemistry, Louisiana State University, Baton Rouge, Louisiana 70803, and Department of Chemistry, University of Houston, Houston, Texas 77204

Received May 24, 2005

The high-yield preparation of metallo-benzoylbiliverdins **9**, **10**, and **11** from either oxidation of dodeca-substituted porphyrin **6** in the presence of $NaNO_2$/TFA and air followed by metalation or by reaction of the Ni(II) or Cu(II) complexes of **6** with *m*-chloroperoxybenzoic acid in pyridine under air is reported. The X-ray structures of complexes **9** and **10** and the electrochemistry and spectroelectrochemistry of metallo-benzoylbiliverdins **9**–**11** are presented and discussed.

Introduction

Metalloporphyrins are subject to oxidation at both the metal center and the porphyrin ligand to form either metal- or porphyrin-centered oxidation products.[1] A number of factors contribute to the preferential site of oxidation including the electronegativity and oxidation state of the central metal,[2] the nature of peripheral substituents on the porphyrin macrocycle,[3] the presence and nature of metal axial ligand(s),[4] the medium,[5] and the temperature.[6] The oxidative cleavage of porphyrin macrocycles is an important reaction that mimics the natural processes of heme catabolism,[7] chlorophyll degradation,[8] and formation of algae biliproteins.[9] The in vivo cleavage of heme **1**, catalyzed by the enzyme heme oxygenase, occurs selectively at the meso α carbon to form verdoheme **2** via a meso-hydroxyheme, which reacts with a second molecule of oxygen to produce biliverdin IXα (**3**), after loss of the meso α carbon as CO and demetalation (Scheme 1).[10] The regioselectivity of heme cleavage by heme oxygenase is probably controlled by both electronic and steric effects exerted by the protein.[11] However, the in vitro chemical oxidation of hemin, normally accomplished using O_2−ascorbic acid or O_2−hydrazine in aqueous pyridine (the so-called coupled oxidation)[12−14] produces all four isomeric biliverdins. This process has been widely used as a model of the heme-oxygenase-catalyzed reactions.[15] A variety of other reaction conditions have also been used for the photo and chemical oxidations of porphyrins, including H_2O_2 in pyridine,[16] thallium(III) and cerium(IV) salts,[17] and O_2−NaOMe in methanol/THF.[18] These reactions typically produce formylbiliverdins (e.g., **4**, from magnesium octaethyl-

* To whom correspondence should be addressed.
† Louisiana State University.
‡ University of Houston.

(1) Fuhrhop, J.-H.; Mauzerall, D. *J. Am. Chem. Soc.* **1969**, *91*, 4174−4181.
(2) Buchler, J. W.; Kadish, W.; Smith, P. D. *Struct. Bonding (Berlin)* **1978**, *34*, 79−134.
(3) Kadish, K. M.; Morrison, M. M. *Bioinorg. Chem.* **1977**, *7*, 107−115.
(4) Whitten, D. G.; Meyer, T. J. *J. Am. Chem. Soc.* **1973**, *95*, 5939−5942.
(5) Kadish, K. M.; Bottomley, L. A. *Inorg. Chem.* **1981**, *20*, 1348−1357.
(6) Dolphin, D.; Felton, R. H. *J. Am. Chem. Soc.* **1975**, *97*, 5288−5290.
(7) Ortiz de Montellano, P. R.; Auclair, K. In *The Porphyrin Handbook*; Kadish, K. M., Smith, K. M., Guilard, R., Eds.; Academic Press: Boston, 2003; Vol. 12, pp 183-210.
(8) Kräutler, B, A. In *The Porphyrin Handbook*; Kadish, K. M., Smith, K. M., Guilard, R., Eds.; Academic Press: Boston, 2003; Vol. 13, pp 183−209.
(9) (a) Frankenberg, N.; Lagarias, J. C. In *The Porphyrin Handbook*; Kadish, K. M.; Smith, K. M.; Guilard, R., Eds.; Academic Press: Boston, 2003; Vol. 13, pp 211−235. (b) Gossauer, A. In *The Porphyrin Handbook*; Kadish, K. M.; Smith, K. M.; Guilard, R., Eds.; Academic Press: Boston, 2003; Vol. 13, pp 237−274.
(10) Wilks, A.; Ortiz de Montellano, P. R. *J. Biol. Chem.* **1993**, *268*, 22357−22362.
(11) Hernandez, G.; Wilks, A.; Paolesse, R.; Smith, K. M.; Ortiz de Montellano, P. R.; La Mar, G. N. *Biochemistry* **1994**, *33*, 6631−6641.
(12) Bonnett, R.; McDonagh, A. F. *J. Chem. Soc., Chem. Commun.* **1970**, 237−238.
(13) Bonnett, R.; McDonagh, A. F. *J. Chem. Soc., Perkin Trans. 1* **1973**, 881−888.
(14) Crusats, J.; Suzuki, A.; Mizutani, T.; Ogoshi, H. *J. Org. Chem.* **1998**, *63*, 602−607.
(15) St. Claire, T. N.; Balch, A. L. *Inorg. Chem.* **1999**, *38*, 684.
(16) Bonnett, R.; Dimsdale, M. J. *J. Chem. Soc., Perkin Trans. 1* **1972**, 2540−2548.
(17) Evans, B.; Smith, K. M.; Cavaleiro, J. A. S. *J. Chem. Soc., Perkin Trans. 1* **1978**, 768−773.
(18) Cavaleiro, J. A. S.; Hewlins, M. J. E.; Jackson, A. H.; Neves, M. G. P. M. S. *J. Chem. Soc., Chem. Commun.* **1986**, 142−144.

10.1021/ic050841c CCC: $33.50
Published on Web 01/13/2006

Scheme 1

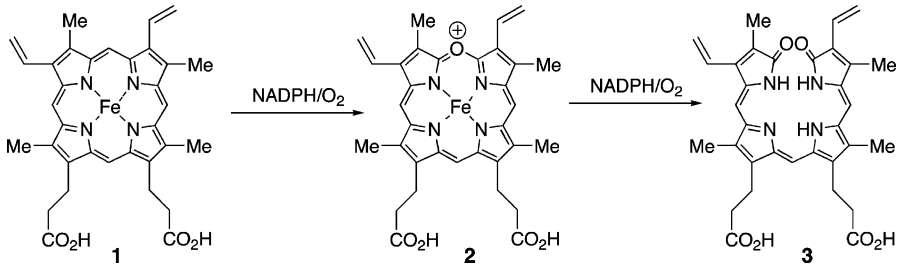

porphyrin),[19−21] biliverdins[12−14] (e.g., **3**, via extrusion of CO) from meso-unsubstituted porphyrins, and aroyl-substituted bilenes from meso-tetraarylporphyrins, such as meso-tetraphenylporphyrin (TPP, **5**). The yields obtained in these reactions are usually low to moderate and depend on the reaction conditions and the presence and nature of the coordinated metal ion.

Herein, we report the high-yield preparation of novel metallo-benzoylbiliverdins (**9**, **10**, and **11**) from the chemical oxidation of dodeca-substituted porphyrin **6** or its Ni(II) and Cu(II) metal complexes **7** and **8** and a study of the electrochemical behavior of the new compounds. Biliverdins have been suggested to have both antioxidant[22] and antiviral activities.[23,24] The study of the chemical and redox properties of model metallo-benzoylbiliverdins, such as **9**−**11** may lead to a better understanding of their possible physiological roles and uncover new applications.[25,26]

The chemical oxidation of the zinc(II) complex of TPP was first reported by Smith and co-workers[27] using thallium(III) salts (trifluoroacetate and nitrate). Subsequently, the Zn(II), Cd(II), bis-Tl(I), and Mg(II) complexes of TPP were ring-opened by photo-oxygenation.[28−30] Under nitrating conditions, using either a mixture of sulfuric and nitric acids[31] or N_2O_4 in organic solvents,[32] TPP (**5**) and its Mg(II) and Zn(II) complexes also produced the corresponding benzoylbiliverdins as a side product. We now demonstrate the preparation of metallo-benzoylbiliverdins **9**−**11** using two different high-yielding routes (Scheme 2): (i) from the

Scheme 2

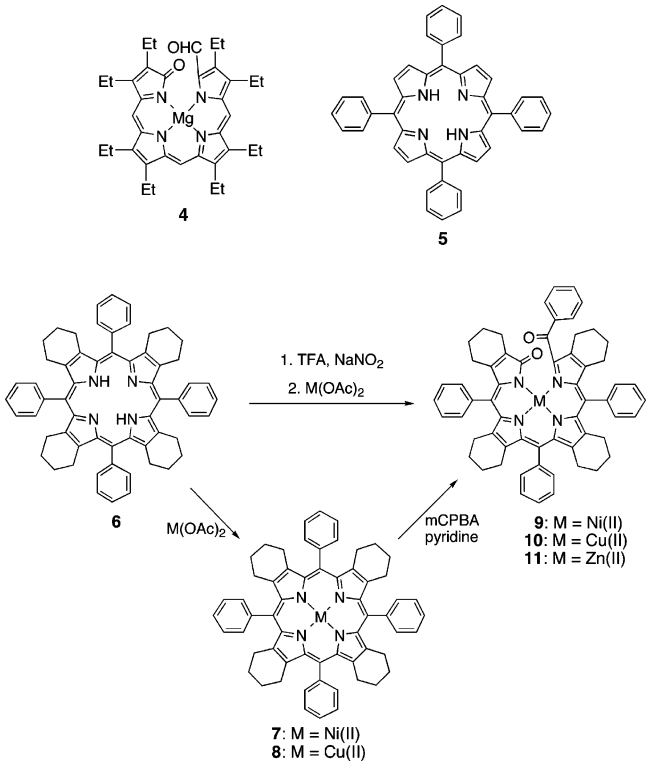

reaction of porphyrin **6** with sodium nitrite in TFA in the presence of oxygen followed by metalation[33] and, for the first time, (ii) from the metal complexes **7** and **8** by reaction with *m*-chloroperoxybenzoic acid (mCPBA) in pyridine and in the presence of oxygen. The oxidation of heme and other iron porphyrins using mCPBA is known to generate iron-oxo species, which catalyze the oxidation of various substrates, such as alkenes and alkanes.[34] However, to the best of our knowledge, mCPBA has never been reported to open the porphyrin macrocycle leading to metallo-biliverdins. The electrochemistry of this class of compounds has not been previously studied and is now described in the present manuscript.

Experimental Section

Alumina (Brockmann EM Separations Grade III) was used for column chromatography. Analytical thin-layer chromatography (TLC) was performed using Merck Sorbent Technologies 60 F254 silica gel (precoated sheets, 0.2 mm thick). The syntheses were

(19) Fuhrhop, J.-H.; Mauzerall, D. *Photochem. Photobiol.* **1971**, *13*, 453−458.
(20) Wasser, P. K. W.; Fuhrhop, J.-H. *Ann. NY Acad. Sci.* **1973**, *206*, 533−547.
(21) Fuhrhop, J.-H.; Wasser, P. K. W.; Subramanian, J.; Schrader, U. *Liebigs Ann. Chem.* **1974**, 1450−1466.
(22) Stocker, R.; Yamamoto, Y.; McDonagh, A. F.; Glazer, A. N. Ames, B. N. *Science* **1987**, *235*, 1043−1046.
(23) Nakagami, T.; Taji, S.; Takahashi, M.; Yamanishi, K. *Microbiol. Immunol.* **1992**, *36*, 381−390.
(24) Mori, H.; Otake, T.; Morimoto, M.; Ueba, N.; Kunita, N.; Nakagami, T.; Yamasaki, N.; Taji, S. *Jpn. J. Cancer Res.* **1991**, *51*, 755−757.
(25) Lord, P. A.; Olmstead, M. M.; Balch, A. L. *Inorg. Chem.* **2000**, *39*, 1128−1134.
(26) Attar, S.; Balch, A. L.; Van Calcar, P. M.; Winkler, K. *J. Am. Chem. Soc.* **1997**, *119*, 3317−3323.
(27) Evans, B.; Smith, K. M.; Cavaleiro, J. A. S. *Tetrahedron Lett.* **1976**, *52*, 4863−4866.
(28) Smith, K. M.; Brown, S. B.; Troxler, R. F.; Lai, J.-J. *Tetrahedron Lett.* **1980**, *21*, 2763−2766.
(29) Smith, K. M.; Brown, S. B.; Troxler, R. F.; Lai, J.-J. *Photochem. Photobiol.* **1982**, *36*, 147−152.
(30) Matsuura, T.; Inoue, K.; Ranade, A. C.; Saito, I. *Photochem. Photobiol.* **1980**, *31*, 23−26.
(31) Johnson, A. W.; Winter, M. *Chem. Ind.* **1975**, *8*, 351.
(32) Catalano, M. M.; Crossley, M. J.; Harding, M. M.; King, L. G. *J. Chem. Soc., Chem. Commun.* **1984**, 1535−1536.
(33) Ongayi, O.; Fronczek, F. R.; Vicente, M. G. H. *Chem. Commun.* **2003**, 2298−2299.
(34) Nam, W.; Lim, M. H.; Lee, H. J.; Kim, C. *J. Am. Chem. Soc.* **2000**, *122*, 6641−6647.

monitored by TLC and spectrophotometry. The electronic absorption spectra were measured in dichloromethane solution using a Perkin-Elmer Lambda 35 UV−vis spectrophotometer. Melting points were measured on a MELT-TEMP apparatus. ^{1}H NMR spectra were obtained in $CDCl_3$ or CD_2Cl_2, using a Bruker 250 or 400 MHz spectrometer; chemical shifts are expressed in ppm relative to TMS (0 ppm) and residual $CHCl_3$ (7.26 ppm). Low-resolution mass spectra were obtained at the Mass Spectrometry Facility at LSU and HRMS at the Ohio State University. Benzaldehyde, BF_3·OEt_2, dichlorodicyanobenzoquinone (DDQ), mCPBA, and the metal acetates were purchased (Aldrich) and used without further purification. Benzonitrile (PhCN) was obtained from Fluka or Aldrich and distilled over P_2O_5 under vacuum prior to use. Tetra-*n*-butylammonium perchlorate (TBAP) was purchased from Sigma or Fluka, recrystallized from ethyl alcohol, and dried under vacuum at 40 °C for at least 1 week prior to use. All solvents were dried and purified according to literature procedures.

Cyclic voltammetry was carried out using an EG&G Princeton Applied Research (PAR) 173 potentiostat/galvanostat. A homemade three-electrode cell was used for cyclic voltammetric measurements and consisted of a platinum button or glassy carbon working electrode, a platinum counter electrode, and a homemade saturated calomel reference electrode (SCE). The SCE was separated from the bulk of the solution by a fritted glass bridge of low porosity, which contained the solvent/supporting electrolyte mixture. Thin-layer UV−vis spectroelectrochemical experiments were performed with a home-built thin-layer cell. Potentials were applied and monitored with an EG&G PAR Model 173 potentiostat. Time-resolved UV−vis spectra were recorded with a Hewlett-Packard Model 8453 diode array spectrophotometer.

5,10,15,20-Tetraphenyl-2:3,7:8,12:13,17:18-butanoporphyrin (6). 6 was prepared as described in the literature.[35,36] Freshly distilled dry dichloromethane (106 mL) was added to a round-bottom flask, fitted with a reflux condenser, under argon. 3:4-Butanopyrrole (0.13 g, 1.06 mmol) and benzaldehyde (0.11 mL, 1.06 mmol) were added, and the solution was stirred at room temperature under a slow, steady stream of argon for 15 min. The flask was then shielded from ambient light, and BF_3·OEt_2 (0.02 mL, 0.106 mmol) was added. This mixture was then stirred for 1 h at room temperature. DDQ (1.15 g, 5.10 mmol) was added to the reaction flask, and the final solution turned dark pink instantly. This solution was refluxed under argon for 1 h to give a dark green solution. The solvent was reduced to dryness under vacuum, and the resulting residue purified by alumina column chromatography using 2% methanol in dichloromethane for elution. Recrystallization from hot methanol gave purple crystals of the title porphyrin (0.17 g, 77% yield). ^{1}H NMR ($CDCl_3$, with 1 drop of *d*-TFA) 8.42 (s, 8 H, *o*-ArH) 7.91 (s, 12 H, *p*- and *m*-ArH) 2.52, 2.04, 1.79, 1.71 (broad s, 8 H each, CH_2) −0.51 (s, 4H, NH). UV−vis (dication, CH_2Cl_2) λ_{max} 459 (214 200), 612 (13 000), 670 (25 000) nm. MS (MALDI) *m*/*z* 831.75 $(M + H)^+$.

Nickel(II) Benzoylbiliverdin (9). From Porphyrin 6. Porphyrin **6** (100 mg, 0.12 mmol) was dissolved in 3 mL of TFA, and $NaNO_2$ (33 mg, 0.48 mmol) was added to the solution with stirring under air at room temperature for 3 min. The reaction was quenched by being poured into 50 mL of water followed by extraction with dichloromethane (6 × 25 mL). The organic layers were washed with saturated aqueous $NaHCO_3$ (2 × 100 mL), then with water (100 mL), and dried over anhydrous Na_2SO_4. The solvent was removed under vacuum, and the residue was purified by column chromatography on alumina, using a gradient elution starting with pure dichloromethane. With 2% methanol in dichloromethane, the metal-free benzoylbiliverdin was collected in an ∼3:1 ratio of the hydrated forms. For the main conformer (violet), mp = 194−196 °C, UV−vis (CH_2Cl_2) λ_{max} 341 nm (19,200), 574 (41,100), ^{1}H NMR (CD_2Cl_2) 11.62, 11.27 (each s, 2 H, NH), 9.00 (s, 1 H, NH), 7.62−7.57 (d, 2 H, *o*-ArH), 7.51−7.35 (m, 18 H, ArH), 6.01 (s, 1 H, OH), 3.8−3.6 (m, 2 H, CH_2), 2.49−1.20 (m, 30 H, CH_2), HRMS *m*/*z* 903.4224 (M + Na); for the pink conformer, mp= 170−173 °C, UV−vis (CH_2Cl_2) λ_{max} 341 (21 700), 508 (13 800) nm, ^{1}H NMR (CD_2Cl_2) 12.57, 9.46 (each s, 2 H, NH), 7.56−7.18 (m, 20 H, ArH), 4.13 (s, 1 H, OH), 3.7 (s, 1 H, NH), 2.41−1.32 (m, 32 H, CH_2), HRMS *m*/*z* 903.4249 (M + Na). The hydrated benzoylbiliverdins were dissolved in toluene (20 mL), and an excess of nickel(II) acetate (24 mg, 0.1 mmol) was added to the solution with stirring. The final mixture was refluxed for 24 h then cooled to room temperature, and the solvent was removed under vacuum. Purification was performed on an alumina plug to remove excess metal acetate, followed by alumina column chromatography using 3:1 dichloromethane/petroleum ether for elution. The product was collected and recrystallized from dichloromethane/methanol to give the title biliverdin (84 mg) in 76% yield.

From the Ni(II) Complex 7.[33] To a stirred solution of complex **7** (20 mg, 0.023 mmol) in pyridine (3 mL) was added mCPBA (30 mg, 0.17 mmol). After 30 min, the solution was evaporated under reduced pressure and the residue was dissolved in dichloromethane and washed with saturated aqueous $NaHCO_3$. Purification as described above yielded **9** (15 mg) in 82% yield. mp = 245−247 °C. UV−vis (CH_2Cl_2) λ_{max} 318 (28 900), 439 (23 500), 802 (9800) nm. ^{1}H NMR ($CDCl_3$, with 1 drop of *d*-TFA) 8.04−7.21 (m, 20 H, ArH), 2.39−1.10 (m, 32 H, CH_2). ^{13}C NMR ($CDCl_3$) 189.3, 181.8, 162.5, 159.1, 149.8, 149.3, 146.4, 145.1, 142.9, 141.9, 140.3, 140.0, 139.5, 138.3, 134.6, 134.5, 133.2, 132.5, 132.3, 131.4, 130.2, 130.0, 129.9, 129.8, 129.6, 129.5, 129.2, 128.3, 32.5, 31.2, 27.5, 27.3, 27.0, 26.5, 26.1, 25.9, 25.8, 24.8, 24.7, 24.5, 24.3, 24.2, 22.6, 15.6. MS (ESI) *m*/*z* 918.9 (M^+). HRMS (ESI) for $C_{60}H_{52}N_4NiO_2$ + Na: calcd 941.3341, found 941.3353. Anal. Calcd for $C_{60}H_{52}N_4NiO_2$: C 72.70, H 6.11, N 5.66. Found: C 73.19, H 6.14, N 5.25.

Copper(II) Benzoylbiliverdin (10). From Porphyrin 6. The metal-free benzoylbiliverdin prepared as described above (100 mg, 0.12 mmol) was dissolved in toluene (20 mL), and copper(II) acetate (239 mg, 1.2 mmol) was added to the solution with stirring. The final mixture was refluxed for 8 h, cooled to room temperature, and the solvent was then removed under vacuum. Purification was first performed on an alumina plug to remove excess metal acetate followed by alumina column chromatography using 3:1 dichloromethane/petroleum ether for elution. The main band was collected and recrystallized from dichloromethane/methanol to give the title biliverdin (80 mg) in 75% yield.

From the Cu(II) Complex 8. Compound **8** was prepared by insertion of Cu(II) into porphyrin **6**, using copper(II) acetate in methanol/chloroform. To a stirred solution of **8** (20 mg, 0.022 mmol) in pyridine (3 mL) was added mCPBA (30 mg, 0.17 mmol). After 30 min, the solvent was evaporated under reduced pressure and the residue was dissolved in dichloromethane and washed with saturated aqueous $NaHCO_3$. Purification as described above yielded **10** (16 mg) in 87% yield. mp = 262−265 °C. UV−vis (CH_2Cl_2) λ_{max} 326 (28 200), 420 (24 200), 481 (28 400), 806 (10 400) nm. MS (ESI) *m*/*z* 924.63 (M^+). HRMS (ESI) for $C_{60}H_{52}CuN_4O_2$ + Na: calcd 946.3284, found 946.3284. Anal. Calcd for $C_{60}H_{52}CuN_4O_2$: C 73.67, H 5.98, N 5.73. Found: C 73.86, H 5.81, N 5.28

(35) Medforth, C. J.; Berber, M. D.; Smith, K. M.; Shelnutt, J. A. *Tetrahedron Lett.* **1990**, *31*, 3719−3722.
(36) Barkigia, K. M.; Renner, M. W.; Furenlid, L. R.; Medforth, C. J.; Smith, K. M.; Fajer, J. *J. Am. Chem. Soc.* **1993**, *115*, 3627−3635.

Table 1. Crystal Data, Data Collection, and Refinement Parameters

compound	**9**	**10**
formula	$2(C_{60}H_{52}N_4NiO_2)0.3(CHCl_3)\cdot MeOH$	$C_{60}H_{52}CuN_4O_2\cdot CH_2Cl_2$
color/shape	brown/fragment	dark brown/parallelepiped
fw	2229.7	1009.5
cryst syst	triclinic	triclinic
space group	$P\bar{1}$	$P\bar{1}$
temp, K	105	105
cell constants		
a, Å	14.932(2)	12.989(3)
b, Å	17.009(2)	14.384(3)
c, Å	22.907(3)	14.553(3)
α, deg	70.580(5)	86.078(8)
β, deg	73.315(5)	82.261(7)
γ, deg	88.440(6)	64.438(9)
V, Å^3	5240.9(12)	2430.4(9)
formula units/unit cell	2	2
D_{calcd}, g cm^{-3}	1.413	1.380
μ_{calc}, cm^{-1}	6.51	6.10
transm. coeff	0.823−0.937	0.890−0.941
diffractometer/scan	Nonius KappaCCD/*ω*	Nonius KappaCCD/*ω*
radiation, graphite monochr.	Mo Kα ($\lambda = 0.71073$ Å)	Mo Kα ($\lambda = 0.71073$ Å)
max cryst dimens, mm^3	0.10 × 0.15 × 0.22	0.10 × 0.20 × 0.25
reflns measured	101 183	49 846
R_{int}	0.058	0.052
independent reflns	21 712	12 459
2*θ* range, deg	$5.0 < 2\theta < 53.0$	$5.6 < 2\theta < 57.4$
range of *h,k,l*	±18, ±21, ±28	±17, ±19, ±19
reflns observed	14 056	8366
criterion for observed	$I > 2\sigma(I)$	$I > 2\sigma(I)$
data/params	21 712/1334	12 459/632
R (obs)	0.068	0.057
R (all data)	0.119	0.103
R_w, F^2(all data)	0.164	0.142
GOF	1.017	1.037
max resid. peaks (e·Å^{-3})	1.50, −1.74	0.84, −1.20

Zinc(II) Benzoylbiliverdin (11). The metal-free benzoylbiliverdin prepared as described above (100 mg, 0.12 mmol) was dissolved in $CHCl_3$ (20 mL), and a saturated solution of zinc(II) acetate in methanol (5 mL) was added to the solution with stirring. The final mixture was refluxed for 8 h, cooled to room temperature, and the solvent was removed under vacuum. The residue was redissolved in dichloromethane (20 mL), and this solution was washed once with saturated aqueous $NaHCO_3$ (100 mL) and once with water (100 mL) before being dried over anhydrous $NaSO_4$. Recrystallization from dichloromethane/methanol gave the title biliverdin (66 mg) in 60% yield. mp = 174−177 °C. UV−vis (CH_2Cl_2) λ_{max} 329 (21 900), 446 (17 200), 752 (6300) nm. ^{1}H NMR ($CDCl_3$) 7.90−7.25 (m, 20 H, ArH), 2.40−1.30 (m, 32 H, CH_2). HRMS for $C_{60}H_{52}N_4O_2Zn$: calcd 925.3460, found 925.3473.

X-ray Data Collection and Structure Determination. Intensity data were collected for solvates of compounds **9** and **10** using graphite-monochromated Mo Kα radiation ($\lambda = 0.71073$ Å) on a Nonius KappaCCD diffractometer fitted with an Oxford Cryostream cooler. Data reduction included absorption corrections by the multiscan method. Crystal data and experimental details are given in Table 1. Structures were solved by direct methods and refined by full-matrix least squares, using SHELXL97.[37] C−H hydrogen atoms were treated as riding in idealized positions. Compound **9** has two independent Ni complexes in the asymmetric unit, one of which has a disorder of one of its cyclohexene rings. In that ring, the two C atoms opposite the double bond take on two conformations with approximately 2:1 population. All residual electron density peaks greater than 1 e·Å^{-3} were located near heavy-atom positions.

Results and Discussion

Porphyrin **6** was synthesized in 77% yield by condensation of 4,5,6,7-tetrahydroisoindole with commercially available benzaldehyde, as previously reported.[35] The precursor 4,5,6,7-tetrahydroisoindole was obtained via Barton−Zard condensation using 1-nitrocyclohexene and ethyl isocyanoacetate in 80−92% yield followed by basic hydrolysis and decarboxylation in 70−85% yield. Because of the core-deformation from planarity in dodeca-substituted porphyrins, these compounds generally have lower oxidation potentials compared with their related octa- and tetra-substituted porphyrins.[31] Thus, the chemical oxidation of porphyrin **6** was accomplished under mild conditions, by adding 6 equiv of $NaNO_2$ to a concentrated solution of **6** in TFA under air, at room temperature.[33] Under similar conditions TPP is mainly nitrated at the para positions of the meso phenyl groups.[38] The green color of the acidic reaction mixture immediately changed to brown. After 10 min, the reaction was quenched with water and neutralized with aqueous sodium bicarbonate solution. The major purple product was isolated in 77% yield, along with 6% recovered starting material and trace amounts of polynitrated products. When this procedure was performed under an inert atmosphere of argon, only starting material **6** was recovered, indicating that air oxygen is essential and is probably added to one of the porphyrin meso positions. In addition, when the reaction was performed using dichlo-

(37) Sheldrick, G. M. *SHELXL97: Program for the Refinement of Crystal Structures*; University of Göttingen: Göttingen, Germany, 1997.

(38) Luguya, R.; Jaquinod, L.; Fronczek, F. R.; Smith, K. M.; Vicente, M. G. H. *Tetrahedron* **2004**, *60*, 2757−2763.

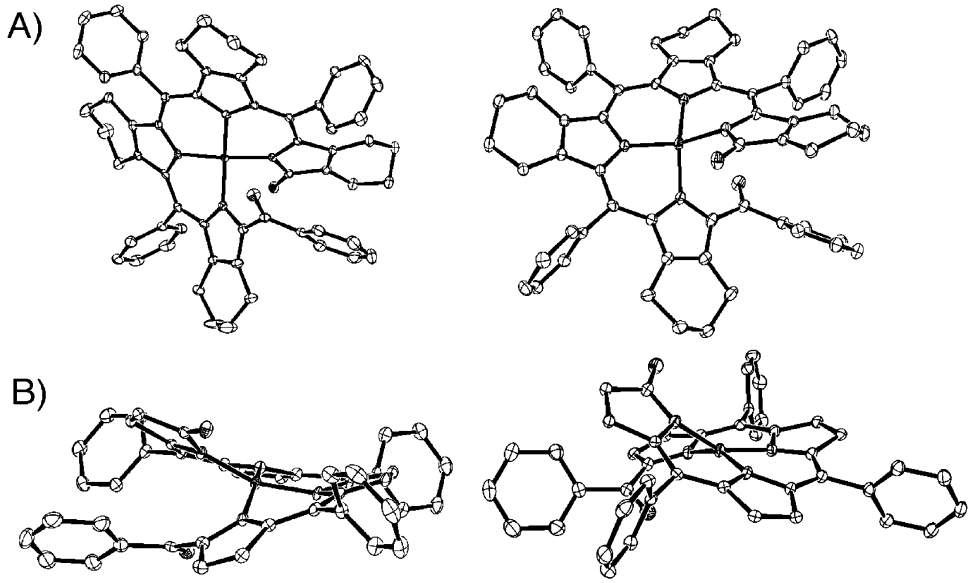

Figure 1. Molecular structures of metallo-benzoylbiliverdins **9** (left) and **10** (right). (A) Top view (hydrogen atoms were omitted for clarity); (B) side view showing square planar distortion (hydrogen and butano carbon atoms were removed for clarity).

romethane as a solvent and a catalytic amount of TFA, or in the absence of TFA, only starting material **6** was recovered. When a radical scavenger (2,6-di-*tert*-butyl-4-methylphenol) was added to the reaction mixture, the ring-opening reaction was completely inhibited. These results suggest that the porphyrin macrocycle is initially oxidized to the corresponding π-cation radical by NO^+, and upon reaction with air oxygen, ring opening occurs, relieving steric strain. The metallo-benzoylbiliverdins **9**−**11** were prepared by treating the conformationally flexible metal-free, ring-opened product with the appropriate metal salts. Both nickel(II) and copper-(II) were inserted in refluxing toluene using the corresponding metal acetates. On the other hand, zinc(II) was inserted using chloroform as the solvent and a saturated solution of zinc(II) acetate in methanol. During the metalation reaction with copper(II) and nickel(II) acetate, a deep blue intermediate complex with a strong absorption at λ_{max} 650 nm was formed. The ^{1}H NMR spectrum of this intermediate showed one broad singlet N−H peak at 8.95 ppm, along with multiple peaks in the aromatic region, and the MALDI-MS showed a molecular ion at 936.3. These results suggest that the metal ion initially coordinates to only three nitrogens and the oxygen of the benzoyl group, in agreement with observations of Callot and co-workers[39] for a nickel and copper complex of a TPP derivative. Further heating in the presence of the metal salt leads to complete disappearance of the blue intermediate and formation of the metallo-benzoylbiliverdins in nearly quantitative yield from the metal-free biliverdin.

The Ni(II) and Cu(II) benzoylbiliverdins were also obtained in a single step, by treating the metal complexes **7** and **8** with mCPBA in pyridine, in the presence of air oxygen. When the reaction was performed under argon, again, no metallobiliverdins were detected by either TLC or spectrophotometry. We believe that mCPBA initially oxidizes porphyrins **7** and **8** to the corresponding porphyrin-cation radicals, which then react with air oxygen to produce metallo-benzoylbiliverdins **9** and **10** in high yield. Since the Zn(II) complex of porphyrin **6** is easily demetalated, biliverdin **11** was prepared in higher yield by zinc(II) insertion into the metal-free benzoylbiliverdin rather than by the mCPBA route. Complex **11** was found to be readily demetalated under acidic conditions, in contrast with the nickel(II) and copper-(II) derivatives **9** and **10**.

The Zn(II) and Ni(II) benzoylbiliverdins had similar ^{1}H NMR spectra, showing two distinct sets of doublets, downfield shifted between 8.04 and 7.72 ppm, corresponding to the ortho aromatic protons of the benzoyl group. The remaining aromatic protons appeared upfield, clustered between 7.64 and 7.21 ppm. A sharp singlet corresponding to two CH_2 protons of the cyclohexenyl ring adjacent to the benzoyl group appeared downfield at about 2.4 ppm, and the remaining CH_2 cyclohexenyl protons appeared as a complex set of peaks between 2.2 and 1.1 ppm. The ^{13}C spectra of metallobenzoylbiliverdins **9** and **11** showed, as expected, two carbonyl resonances at about 189 and 182 ppm, the aromatic carbons appeared between 162 and 128 ppm, and the CH_2 between 32 and 16 ppm. Suitable crystals for X-ray analysis of complexes **9** and **10** were grown from slow diffusion of chloroform into methanol, and the molecular structures of these compounds are shown in Figure 1. Compound **9** has two independent molecules in the asymmetric unit, and only one of the molecules is shown in the figure. We have recently published the structure of benzoylbiliverdin **9**[33] as a mixed CH_2Cl_2/MeOH/H_2O solvate. That structure had only one independent benzoylbiliverdin molecule but suffered from considerable solvent disorder problems, and the precision of the determination was somewhat lower than the $CHCl_3$/MeOH solvate reported here. In both complexes **9** and **10**, the metal atoms have tetrahedrally distorted square planar geometries enforced by the oxidized nonmacrocyclic nature of the ligand. In the Ni(II) complex,

(39) Jeandon, C.; Krattinger, B.; Ruppert, R.; Callot, H. J. *Inorg. Chem.* **2001**, *40*, 3149−3153.

Table 2. Half-wave Potentials (V vs SCE) of Complexes **7**−**11** in PhCN, 0.1 M TBAP

	oxidation			reduction			
compound	third	second	first	first	second	third	$\Delta E_{1/2}$[a]
(BV)Ni **9**	−	1.30[b]	0.80	−0.79	−1.30[b]	−	1.59
(BV)Cu **10**	1.80[b]	1.25	0.81[b]	−0.65	−1.08	−1.53	1.46
(BV)Zn **11**	1.26[b]	1.10[b]	0.72[b]	−0.49	−0.63	−1.16[b]	1.21
(TPBP)Ni **7**	1.64	0.93	0.73	−1.49	−1.83	−	2.22
(TPBP)Cu **8**	−	1.01	0.55	−1.50	−1.90[b]	−	2.05

[a] $\Delta E_{1/2}$ = the potential difference between the first oxidation and first reduction. [b] Peak potential at a scan rate of 0.1 V/s.

the N atoms at the oxygenated ends of the benzoylbiliverdin ligand lie out of the plane defined by the Ni and the two central N atoms by 0.635(4) and −0.716(4) Å (0.677(4) and −0.693(4) Å for the second molecule). The distortion is slightly larger for the Cu complex, with out-of-plane deviations of 0.759(3) and −0.884(3) Å for those N atoms. The Ni−N bond lengths fall within the range 1.845(3)−1.868(3) Å for the Ni(II) complex and 1.924(2)−1.932(2) Å for the Cu(II) complex. The benzoyl O atom also forms a longer intramolecular interaction with the metal, having M···O distances of 2.973(4) and 3.076(4) Å for M═Ni and 2.933(3) Å for M═Cu. Although to date we have not obtained crystals of the Zn(II) complex **11** suitable for X-ray determination of its structure, we believe that this complex is significantly more distorted than the Ni(II) and Cu(II) derivatives. This conclusion is based on the following observations: (1) Unlike **9** and **10**, the Zn(II) complex **11** readily undergoes demetalation under mildly acidic conditions, such as during purification using alumina or silica gel chromatography. (2) The Zn(II) complex **11** is significantly less stable than **9** or **10**, decomposing upon storage under air in a few days. In contrast, the Ni(II) and Cu(II) complexes are very stable under the same conditions even after several months. (3) The UV−vis spectrum of the Zn(II) complex **11** in CH_2Cl_2 shows a blue-shifted long-wavelength band at 752 nm compared with the corresponding absorptions for the Ni (802 nm) and the Cu (806 nm) complexes. (4) The electrochemistry of the Zn(II) complex is distinctly different from that of the Ni(II) and Cu(II) derivatives (vide infra). These observations strongly suggest a different conformation for the Zn(II) derivative from those shown in Figure 1 for the Ni(II) and Cu(II) complexes; the ring-opened ligand is able to distort a lot more than a porphyrin macrocycle in order to accommodate the larger and possibly penta- or hexacoordinated Zn ion.

Electrochemistry and Spectroelectrochemistry. Cyclic voltammetry of metallo-benzoylbiliverdins **9**−**11** was carried out in PhCN containing 0.1 M TBAP. The half-wave potentials of these complexes are summarized in Table 2. Each compound undergoes two or three reductions in PhCN, 0.1 M TBAP. The first reduction for all three compounds **9**−**11** is reversible and is located at $E_{1/2} = -0.79$ V for Ni(II), −0.65 V for Cu(II) and −0.49 V for Zn(II), respectively. The second reduction of **9**−**11** ranges from −1.30 to −0.63 V (Table 2).

Nickel(II) benzoylbiliverdin [(BV)Ni] undergoes two reductions, the second of which is not reversible (Figure 2a).

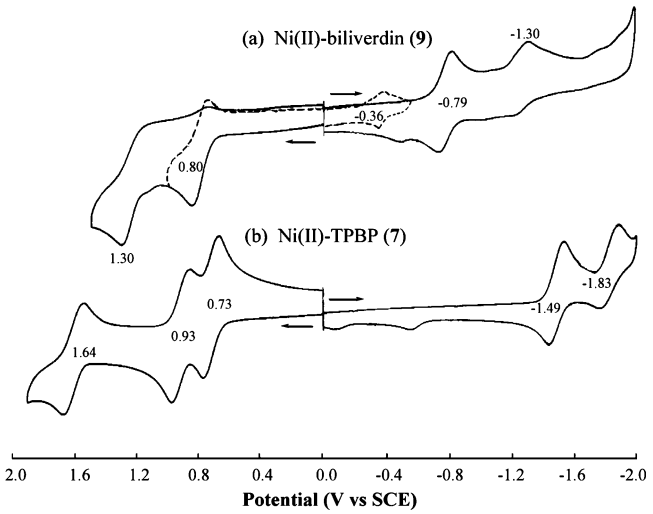

Figure 2. Cyclic voltammograms of Ni(II) benzoylbiliverdin **9** and Ni(II) porphyrin **7** in PhCN, 0.1 M TBAP.

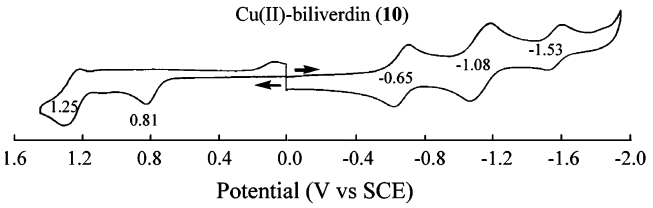

Figure 3. Cyclic voltammogram of Cu(II) benzoylbiliverdin **10** in PhCN, 0.1 M TBAP.

This result suggests that the second reduction of compound **9** is coupled with one or more subsequent chemical reactions. The electrochemical behavior of (BV)Ni **9** is different from that of the Ni(II) complex **7** [(TPBP)Ni][40] which shows normal porphyrin electrochemical properties (see Figure 2b). The Cu(II) complex **8** [(TPBP)Cu] also shows normal porphyrin behavior. The compound is reduced at $E_{1/2} = -1.50$ V and $E_{pc} = -1.90$ V for a scan rate of 0.1 V/s and is oxidized at $E_{1/2} = 0.55$ and 1.01 V vs SCE in PhCN, 0.1 M TBAP. In contrast, three reversible reductions are located at $E_{1/2} = -0.65$, −1.08, and −1.53 V are observed for the copper(II) benzoylbiliverdin, [(BV)Cu] **10**, in PhCN (see Figure 3). The electrochemical behavior of the zinc(II) benzoylbiliverdin, [(BV)Zn] **11**, is similar to that of the copper(II) complex **10**. However, only the first two reductions of compound **11** are reversible (Table 3).

Up to three oxidations can be observed for complexes **9**−**11** in PhCN containing 0.2 M TBAP. The first oxidation of the Ni(II) complex is located at $E_{1/2} = 0.80$ V, and a small rereduction wave at −0.36 V can be observed in addition to the main anodic process when the potential scan is reversed after the first oxidation (Figure 2a). The first oxidation of the Cu(II) and Zn(II) complexes is irreversible and is located at 0.81 and 0.72 V, respectively (Table 2). The difference of potentials between the first reduction and the oxidation (HOMO−LUMO gap) is 1.59 V for complex **9**, 1.46 V for **10**, and 1.21 V for **11** (Table 2). These values are much

(40) Kadish, K. M.; Van Caemelbecke, E.; Boulas, P.; D'Souza, F.; Vogel, E.; Kisters, M.; Medforth, C. J.; Smith, K. M. *Inorg. Chem.* **1993**, *32*, 4177−4178.

Table 3. UV−vis Spectral Data of M(II) Benzoylbiliverdins **9**−**11** in PhCN, 0.2 M TBAP

			λ_{max}, nm[a]						
M(II)	rxn	E_{app} (V)	Soret region			visible region			
Ni	none	none	326	442					804
	1st ox	+1.00	367	415		552	580	662	720
	2nd ox	+1.50	322	442					779
	1st red	−1.00	331	460		579		774	897
	2nd red	−1.50	330	402	437		626	734	
Cu	none	none	344	422	484			762	814
	1st ox	+1.00	349	415			628[sh]	680	793
	2nd ox	+1.50	352	412		530		680	824
	1st red	−0.90	365	459				790	878
	2nd red	−1.40	315	398	460		645	791	
	3rd red	−1.80	354			599	646		
Zn	none	none	330	455				752	
	1st ox	+0.90	329	455				752	
	2nd ox	+1.20	328	404[sh]	453[sh]		661	739	
	1st red	−0.55	339	437	482[sh]	580	646	752	824
	2nd red	−0.80	347	446			600	647	

[a] sh = shoulder peak.

smaller than the HOMO−LUMO gap (~2.25 V) for generic TPP or OEP complexes.[41]

The plots of the redox potentials as a function of the ratio between the metal ion electronegativity and the radius (EN/ri) for compounds **9**−**11** are given in the Supporting Information (Figure S1). The potentials for the first and second oxidations of the biliverdin complexes increase upon going from Zn to Cu to Ni complex. The electrochemical results indicate that the HOMO orbital energy of the Zn(II) complex is higher than that of the Cu(II) and Ni(II) complexes. The slope of the plot for the first oxidation equals 93 mV, while the slope for the second oxidations is 200 mV. This result suggests that the coordinated metal ion might have a stronger effect on the second oxidation of the biliverdin complexes. When M(II) is varied from Zn to Ni, the first reduction shifts negatively with a slope of −271 mV, while the second reduction exhibits a much larger negative shift of −645 mV. This confirms that the metal ion also has a strong effect on the second reductions of complexes **9**−**11**. A comparison between the slope of the plots for reduction and oxidation of complexes **9**−**11** indicates clearly that the reductions exhibit significant metal ion dependence.

UV−vis spectra for the nickel porphyrin (TPBP)Ni **7** and the Ni(II) biliverdin **9** are presented in Figure 4. A typical porphyrin spectrum with a strong Soret band at 427 nm and two weak visible bands at 545 and 581 nm can be seen for (TPBP)Ni **7** in PhCN. However, Ni(II) biliverdin **9** exhibits only two weak, broad, short-wavelength bands at 326 and 442 nm, and there is a single broad visible band at 804 nm in the same solvent.

Thin-layer UV−vis spectroelectrochemistry was carried out in PhCN containing 0.2 M TBAP. The spectral data obtained upon controlled-potential reduction or oxidation of complexes **9**−**11** are summarized in Table 3 while, the spectral changes obtained for **9**−**11** in PhCN, 0.2 M TBAP are shown in Figures 5−7 and Figure S2 of the Supporting Information.

Upon the first reduction of the Ni(II) complex **9** at −1.00 V, the short-wavelength bands at 326 and 442 nm red-shift

(41) Kadish, K. M. *Prog. Inorg. Chem.* **1986**, *34*, 435−605.

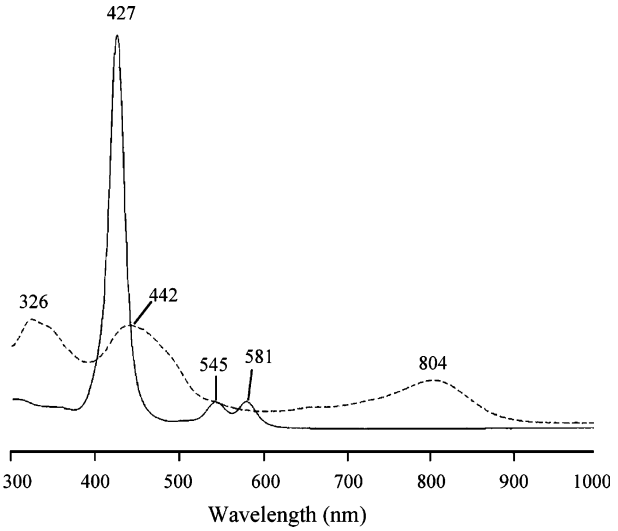

Figure 4. UV−vis spectra (TPBP)Ni **7** (full line) and Ni(II) benzoylbiliverdin **9** (dash line) in PhCN containing 0.2 M TBAP.

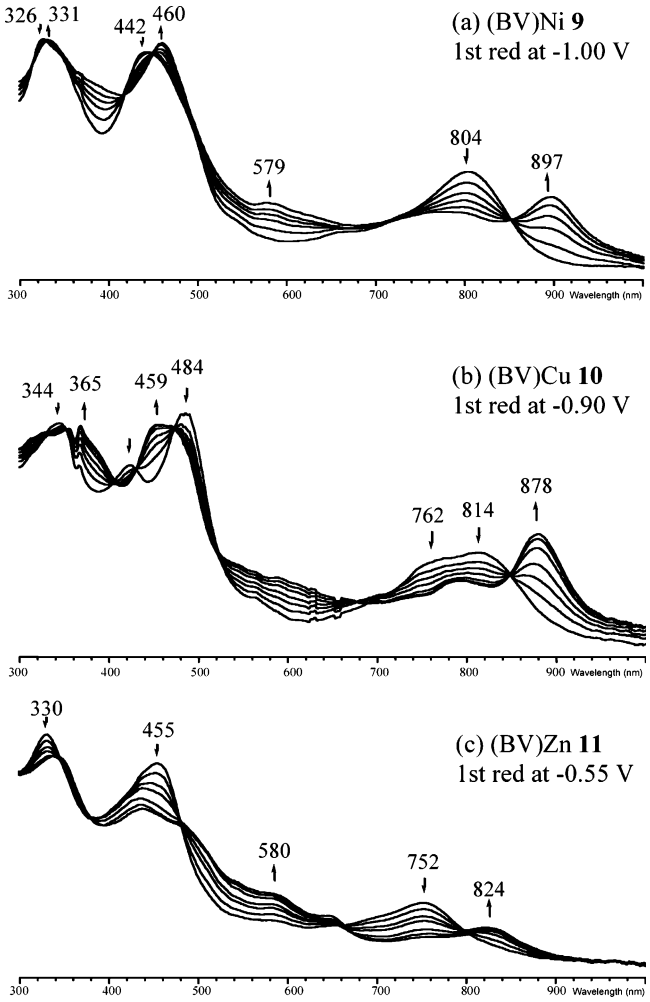

Figure 5. Thin-layer UV−vis spectral changes of M(II) benzoylbiliverdins **9**−**11** obtained upon the controlled-potential reduction in PhCN, 0.2 M TBAP.

to 331 and 460 nm with only slight changes in intensity. The visible band at 804 nm for this complex almost disappears, while a new band at 897 nm grows up during the first controlled-potential reduction in PhCN, 0.2 M TBAP (Figure 5a). Similar spectral changes are observed upon the

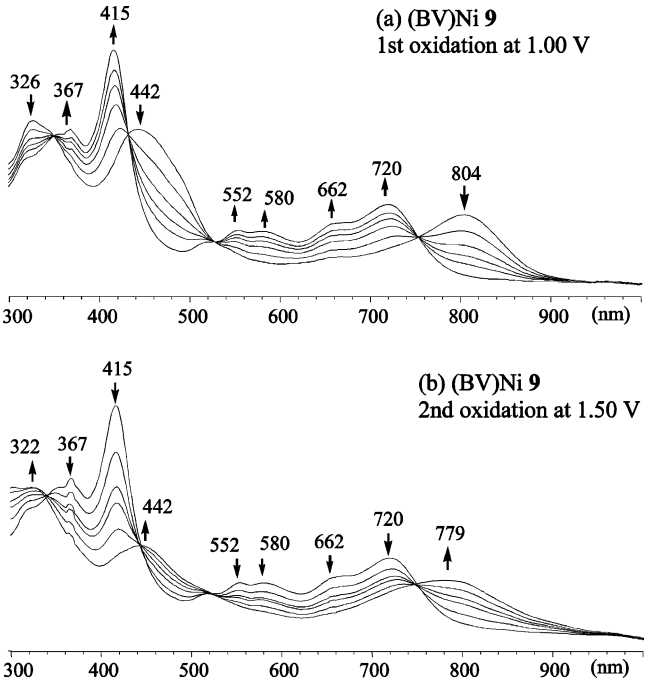

Figure 6. Thin-layer UV−vis spectral changes of Ni(II) benzoylbiliverdin **9** obtained upon the controlled-potential oxidations in PhCN, 0.2 M TBAP.

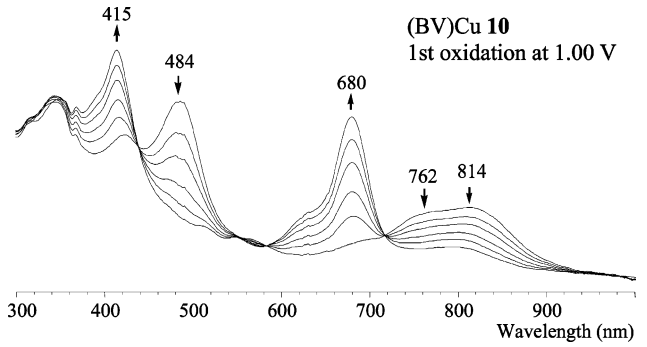

Figure 7. Thin-layer UV−vis spectral changes of Cu(II) benzoylbiliverdin **10** obtained upon the first controlled-potential oxidation in PhCN, 0.2 M TBAP.

first reduction of the Cu(II) complex **10** under the same experimental conditions (Figure 5b). However, the spectral changes for the Zn(II) complex **11** are different from the Ni(II) and Cu(II) derivatives. Here bands at 330 and 455 nm decrease in intensity upon the first reduction at −0.55 V (Figure 5c).

During the first oxidation of the Ni(II) complex **9** at 1.00 V, the absorption bands at 442 and 804 nm disappear while a strong Soret band at 415 nm and four visible bands at 552, 580, 662, and 720 nm appear (Figure 6a). The bands at 415, 552, and 580 nm for the final spectrum of the oxidized species are similar to that of the nickel porphyrin, (TPBP)Ni **7**, which has a Soret band at 427 nm and two visible bands at 545 and 581 nm. Upon further oxidation of **9** at 1.50 V, a spectrum with Soret bands at 322 and 442 nm and a broad visible band at 779 nm was observed which is similar to the neutral spectrum of **9** (Figure 6b). This result suggests that an open-chain structure is re-formed under the experimental conditions.

Spectral changes upon the first oxidation of Cu(II) complex **10** are shown in Figure 7. As is also seen for the Ni(II) complex **9**, a new Soret band at 415 nm appears when the oxidation potential is set at 1.00 V (see Figures 6a and 7). A very strong visible band at 680 nm is also observed upon the first oxidation. This result is different from that of the Ni(II) complex **9**, which has no strong visible bands and only four weak bands in this spectral region.

For the Zn(II) complex **11**, the spectral changes obtained upon the oxidations are totally different from those of Ni(II) and Cu(II) complexes, and this is shown in Figure S2 of the Supporting Information. Upon the first oxidation at 0.90 V, all absorption bands decrease only slightly in intensity and no new bands can be discerned.

Conclusions

Two high-yielding synthetic methods for the preparation of metallo-benzoylbiliverdins have been developed using the chemical oxidation of a dodeca-substituted porphyrin and its Ni(II) and Cu(II) complexes. Benzoylbiliverdins **9** and **10** were prepared in 75−87% overall yields either from porphyrin **6** using $NaNO_2$/TFA and air followed by metalation or from complexes **7** and **8** by reaction with mCPBA/pyridine in the presence of air. The zinc(II) complex **11** was obtained by oxidation of porphyrin **6** followed by metalation due to the instability of the Zn(II) porphyrin in the presence of mCPBA; this route does not depend on the oxidation potential or the stability of the metallo-porphyrin. The molecular structures of complexes **9** and **10** were determined and show significantly distorted square planar geometries for the central metal ions. The electrochemistry and spectroelectrochemistry of metallo-benzoylbiliverdins **9**−**11** are carried out in PhCN contaning 0.1 or 0.2 M TBAP. Up to three reductions and three oxidations are observed. The differences of potentials between the first reduction and the first oxidations range from 1.21 to 1.59 V vs SCE, which is much smaller than the value of 2.25 ± 0.15 V for generic TPP or OEP complexes or 2.05−2.22 V for the two porphyrin complexes **7** and **8** examined in the present study.

Acknowledgment. The research described was supported by the National Science Foundation (Grant No. CHE-304833, M.G.H.V.), the National Institutes of Health (Grant No. EB-002064, K.M.S.), and the Robert A. Welch Foundation (Grant No. E-680, K.M.K.).

Supporting Information Available: X-ray data in CIF format for **9** and **10**, the redox potentials of complexes **9**−**11** in PhCN containing 0.1 M TBAP (Figure S1), and the thin-layer UV−vis spectral changes of Zn-biliverdin **11** obtained upon the first and second oxidations in PhCN, 0.2 M TBAP (Figure S2). This material is available free of charge via the Internet at http://pubs.acs.org.

IC050841C